Liquidlike Order of Charged Rodlike Particle Solutions

Erich E. Maier, Rainer Krause, Martin Deggelmann, Martin Hagenbüchle,* and Reinhart Weber

Fakultät für Physik, Universität Konstanz, Postfach 5560, 7750 Konstanz, FRG

Seth Fraden†

Hochfeld-Magnetlabor, Max-Planck-Institut für Festkörperforschung, 166X, 38042 Grenoble Cedex, France

ABSTRACT: The structural order in the isotropic phase of charged rodlike TMV solutions (length L = 300 nm) has been investigated by static light scattering (SLS) and small-angle neutron scattering (SANS) experiments. We present measurements of the static structure factor $S(q)$ as a function of the ionic strength over the concentration regimes $c < c^*$ and $c > c^*$ (c^* = 1 particle/L^3). SANS results in the semidilute regime $c > c^*$ show that strong interparticle correlations are present even at concentrations as high as $25c^*$, in contrast to results for hard-rod systems. The magnitudes of the correlations depend on both the macroion concentration and the Debye screening length κ^{-1}. As expected the position of the first maximum of $S(q)$ is found to scale with concentration as $q_{max} \sim c^{1/3}$ below the overlap concentration c^* but surprisingly to turn over to a $c^{1/2}$ behavior above c^*. With increasing salt, at constant macroion concentration a decrease in structure is observed and the first-maximum position q_{max} is shifted to larger scattering vectors. In the absence of any adequate theory we compare our results to SLS measurements and HNC calculations of a spherical particle system. The influence of added salt on TMV solutions is examined by Monte Carlo simulations at $c < c^*$.

1. Introduction

Aqueous solutions of charged colloidal particles exhibit a number of order phenomena studied experimentally and theoretically. Due to the long-range Coulombic interaction of the macromolecules which results from negatively charged surface groups and the screening ions, a short-range or liquidlike order is observed,[1-3] equivalent to the nearest-neighbor order of simple liquids.

In solutions of polystyrene *spheres* the influence of the ionic strength and the colloid particle concentration on the liquidlike order is the subject of detailed experimental investigations.[4-6] An adequate intermolecular pair potential is evaluated and provides an excellent agreement of experimental and theoretical static structure factors from which the radial pair distribution function can be calculated. With increasing particle concentration solutions of monodisperse spherical particles are known to crystallize into bcc or fcc lattices with intersphere spacings of many times the particle diameter.[3,7] Much more complicated is the phase diagram of *anisotropic* particle systems. At a critical concentration, as first explained by Onsager,[8] rods interacting with a hard-core potential separate into an isotropic and an anisotropic nematic phase coexisting in equilibrium. The latter phase is characterized by a long-range orientational order and a liquidlike positional order of the rodlike macromolecules. In the case of rodlike polyelectrolytes, such as TMV or fd virus, additionally the effect of the electrostatic interaction has to be taken into account. The isotropic–nematic phase transition of TMV solutions depends on both the particle concentration and the ionic strength. With increasing ionic strength the concentrations of the coexisting isotropic and nematic phase increase, which can be interpreted in terms of an effective diameter and a twisting parameter.[8-12] For the investigations of the liquidlike structure in the semidilute regime the concentration of the coexisting isotropic phase gives the starting concentration of the dilution series to be examined.

Substantial experimental and theoretical investigations of *flexible* linear polyelectrolytes, such as NaPSS, reveal a single broad peak in the scattered intensity in salt-free solutions.[13-15] As the single ion conformation depends on the macroion and salt concentration, the particle form factor is unknown and consequently the static structure factor cannot be derived. Nevertheless, SANS (small-angle neutron scattering), SAXS (small-angle X-ray scattering), and SLS (static light scattering) measurements demonstrate that in the concentration regime where different chains overlap the intensity peak positions shift as $c^{1/2}$. Later, SAXS[13] and SLS[15] provided additional information from which a critical concentration was derived below which the usual $c^{1/3}$ behavior of peak position occurs. A quantitative theory explaining the structural properties of flexible polyelectrolytes is still lacking. Because of the difficulties with linear polyelectrolytes we started experimental investigations on rodlike macromolecules in aqueous solutions by static and dynamic light scattering, which should serve as a link between spherical and linear flexible polyelectrolytes.

The first systems investigated by SLS were isotropic solutions of TMV and fd particles.[16-18] TMV solutions can be monitored below c^* = 1 particle/L^3 only, whereas fd solutions, because of the bigger length of the phages (L = 880 nm), can be investigated mainly above c^*. As a result the concentration regime can be divided into two parts by the overlap concentration c^*. Well below c^* the particles may approximately be considered as interacting charged spheres. Consequently, the static structure factor is expected and is found to be liquidlike; the position q_{max} of its maximum scales with concentration as $q_{max} \sim c^{1/3}$. In contrast, above c^* a $c^{1/2}$ dependence is found. It is claimed that this behavior is a general feature of rodlike particle systems caused by the anisotropic particle geometry. Apart from a few experimental points below c^* for the fd solutions, this is proven for the two different

† Present address: Martin Fisher School of Physics, Brandeis University, Waltham, MA 02254.

macromolecules below and above the critical concentration, respectively.

To test the different scaling of q_{max}, in this paper the rodlike TMV particle is studied in the concentration regime $0.05c^* \leq c \leq 26.5c^*$ ($c^* = 2.45$ mg/mL) by SLS and SANS techniques.

As shown theoretically for spherical particle systems the first maximum position of the static structure factor is shifted to larger scattering vectors as a function of the ionic strength.[19] Up to now, even for spherical particle systems, detailed experimental studies on the screening ion's influence on the structural order are missing. Difficulties arise in adding exact salt concentrations as the formation of the liquidlike order in the very diluted regime requires very low ionic strength solutions ($\approx 10^{-6}$ M). A new closed-tube circuit technique is presented which allows detailed SLS and in the future also SANS measurements of the static structure factor of macroparticle solutions as a function of the electric conductivity. In a first-order approximation the screening ion concentration, which is related to the Debye screening length κ^{-1}, is derived therefrom. Moreover the first-maximum positions as a function of the salt concentration are important to interpret the SANS data.

2. Theoretical Section

2.1. Static Light Scattering.

In a SLS experiment the averaged scattered intensity of a system of N monodisperse interacting particles is described by the Rayleigh–Gans–Debye approximation as

$$I(q) = N V_p^2 b^2 P(q) \, S(q) \tag{1}$$

where V_p is the particle volume and b is proportional to the refractive index difference between the colloidal particles and the solvent. The particle form factor $P(q)$ is due to the intraparticle interferences, and the static structure factor contains information about the structural ordering of the particles.

The virus particles are modeled as rigid rods of length L and vanishing diameter. The positions of the scattering centers are fixed along the particle orientation vector $\vec{u}_i$. For an isotropic solution the particle form factor $P(q)$ is calculated as[20]

$$P(q) = \frac{1}{V_p^2}\langle |\int_{V_p} e^{i\vec{q}\vec{r}}\, d\vec{r}|^2 \rangle = \frac{2}{qL}\int_0^{qL} dz\, \frac{\sin z}{z} - \left(\frac{2}{qL}\sin\left(\frac{qL}{2}\right)\right)^2 \tag{2}$$

The static structure factor depends on both the positions of centers of gravity $\vec{R}_i$ and $\vec{R}_j$ and the mutual orientation of two rods[21]

$$S(q) = 1 + \frac{1}{NP(q)}\langle \sum_{i\neq j}^{N} e^{i\vec{q}(\vec{R}_i-\vec{R}_j)} f_i f_j \rangle \tag{3}$$

with

$$f_i = \frac{\sin(\vec{q}\vec{u}_i L/2)}{\vec{q}\vec{u}_i L/2} \tag{4}$$

where $P(q)$ can also be written as $P(q) = \langle f_i^2 \rangle$. In contrast to spherical particle systems, so far a proper evaluation of the static structure factor by means of integral equation theory is not available if the particles strongly interact. For weakly interacting systems an expression for $S(q)$ is obtained which is an increasing function of q only.[22] The static structure factor of eq 3 is related to the pair distribution function $g(\vec{r},\vec{u}_1,\vec{u}_2)$, i.e., the probability of finding a particle with orientation $\vec{u}_2$ at a distance $\vec{r}$ from

a particle at $\vec{r} = 0$ with orientation $\vec{u}_1$, by[21]

$$S(q) = 1 + \frac{c}{P(q)}\frac{1}{4\pi^2}\int d\vec{u}_1\, d\vec{u}_2\, j_0(\vec{q}\vec{u}_1 L/2)\, j_0(\vec{q}\vec{u}_2 L/2) \times$$
$$\int d\vec{r}\, e^{i\vec{q}\vec{r}}[g(\vec{r},\vec{u}_1,\vec{u}_2) - 1] \tag{5}$$

where $c = N/V$ and

$$j_0(\vec{q}\vec{u}L/2) = \sin(x)/x \tag{6}$$

As shown by eq 5 it is not possible to deduce unequivocally the pair distribution function from the experimental static structure factor. In the case of interacting spheres a position of q_{max} can be associated with a mean distance r_{max} of nearest neighbors.

Regarding our concentration range $0.05c^* \leq c \leq 26c^*$, a useful approximation is possible in the regime $c \ll c^*$ where the mean interparticle distance is much larger than the rod length. Consequently the interaction potential is independent of the particle orientation so that any correlations between the orientation distribution of the particles i and j and their distances $(\vec{R}_i - \vec{R}_j)$ can be neglected, and therefore there is no correlation between $f_i(\vec{q},\vec{u}_i)$ and $f_j(\vec{q},\vec{u}_j)$. Thus

$$S(q) = 1 + \frac{1}{N}\frac{\langle f_i \rangle^2}{\langle f_i^2 \rangle}\langle \sum_{i\neq j}^{N} e^{i\vec{q}(\vec{R}_i-\vec{R}_j)} \rangle \tag{7}$$

$$S(q) = 1 + \frac{\langle f_i \rangle^2}{\langle f_i^2 \rangle}(S_{CG}(q) - 1) \tag{8}$$

Here

$$S_{CG} = 1 + \frac{1}{N}\langle \sum_{i\neq j}^{N} e^{i\vec{q}(\vec{R}_i-\vec{R}_j)} \rangle \tag{9}$$

is the static structure factor of the centers of gravity of the particles. Of course for spherical particles $\langle f_i^2 \rangle = \langle f_i \rangle^2$ and therefore $S_{CG} = S(q)$.

In an isotropic solution of rodlike particles the static structure factor in this approximation is expected to be less pronounced, compared to spherical particle systems, if the particle orientation becomes important to the interparticle pair potential. Since $\langle f_i^2 \rangle \leq \langle f_i \rangle^2$, these deviations in the $S(q)$ behavior increase if the main peak position, with increasing concentration, is shifted to large q values. A more detailed study concerning the particle anisotropy influence is given in our recent publication on fd solutions.[18]

2.2. Small-Angle Neutron Scattering.

In the SANS experiment the coherent scattering rate $I(q)$ is obtained after the usual correction for the background scattering and the incoherent scattering as

$$I(q) = N\left(\frac{d\sigma(q)}{d\Omega}\right)_{coh} \tag{10}$$

N is the particle density and the coherent differential cross section per particle is given by

$$\left(\frac{d\sigma(q)}{d\Omega}\right)_{coh} = \frac{d\sigma_0}{d\Omega}P(q)\, S(q) \tag{11}$$

with

$$\frac{d\sigma_0}{d\Omega} = (\rho_p - \rho_s)^2 V_p^2 \tag{12}$$

where ρ_p and ρ_s are the scattering length densities of the particle and the solvent.

To derive expressions for the particle form factor $P(q)$ and the static structure factor $S(q)$, the rodlike virus has
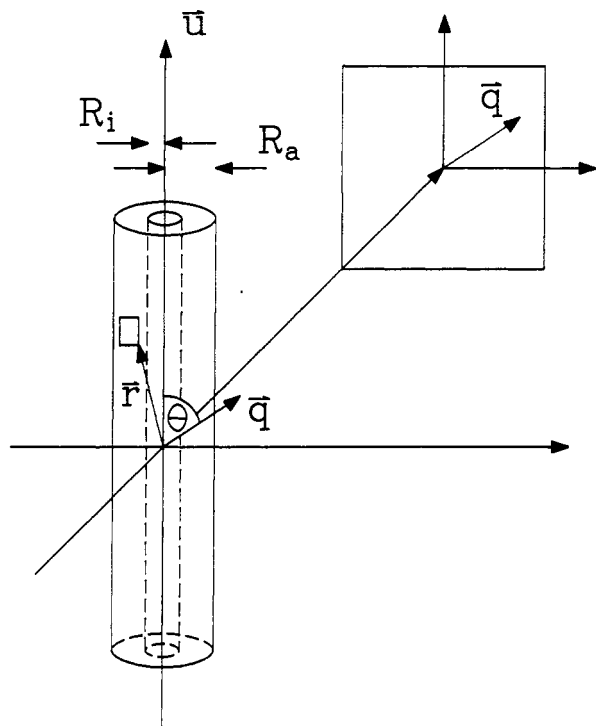
Figure 1. Scattering geometry of the SANS experiments: R_i = inner radius, R_a = outer radius, $\vec{u}$ = direction of the cylinder axis, $\vec{q}$ = scattering vector at the two-dimensional detector area.

to be modeled according to the characteristic length of a SANS experiment. The TMV particle is known to be a hollow cylinder of length L = 300 nm with an inner radius R_i = 2 nm and an outer radius R_a = 9 nm.[23,24] For a homogeneous rod the particle form factor is calculated as

$$P(q) = \langle |f(\vec{q},\vec{u})|^2 \rangle \tag{13}$$

$$f(\vec{q},\vec{u}) = \frac{1}{V_p} \int_{V_p} e^{i\vec{q}\vec{r}} \, d\vec{r} \tag{14}$$

where $\vec{q}$ is the scattering vector at the detector area, $\vec{u}$ is the direction of the cylinder axis as shown in Figure 1, and $f(\vec{q},\vec{u})$ is the form amplitude. In the isotropic phase the particle form factor is numerically calculated by the average over the isotropic orientation distribution of the cylinder axes

$$P(q) = \frac{1}{4\pi} \int_0^{2\pi} d\phi \int_0^\pi d\vartheta \, |f(q\mu)|^2 \sin\vartheta \tag{15}$$

$$P(q) = \int_0^1 d\mu \, |f(q\mu)|^2 \tag{16}$$

with $\mu = \cos\theta$ where θ is the angle between the orientation vector $\vec{u}$ and the scattering vector $\vec{q}$. As no optical birefringence is found in the concentration regime covered by our SANS experiments, long-range orientational ordering can be excluded. An expression for the static structure factor $S(q)$ is then derived from eq 11 using eq 16 for the form factor. But a recent study of the magnetic field induced birefringence in the isotropic phase shows that there are local angular correlations between the rods which depend on the particle and salt concentration.[12] This behavior is confirmed by our MC simulation results on fd particle solutions.[18]

2.3. Monte Carlo Simulations. Monte Carlo (MC) simulations for solutions of charged stiff rods have been performed applying the usual Metropolis algorithm. The

rods are divided into charged spherical segments. On the basis of the so-called one-component macroion fluid model (OCM), the interaction between two rods with the orientations $\vec{u}_i$ and $\vec{u}_j$ and a center of gravity distance $\vec{R}$ is given by the repulsive screened Coulombic potential

$$U(\vec{R},\vec{u}_1,\vec{u}_2) = \sum_{i,j} A_{DLVO} e^{-\kappa r_{ij}} \tag{17}$$

with the repulsive part of the well-known DLVO potential

$$A_{DLVO} = \frac{(Q/n)^{1/2}}{4\pi(1 + \kappa a)^2} e^{2a\kappa} \tag{18}$$

Q is the total charge per rod, n the number of segments, a the hard-core radius of the segments, and r_{ij} the distance between segment i on rod 1 and segment j on rod 2.

The inverse Debye screening length κ^{-1} can be calculated from the counterion plus the added salt concentration

$$\kappa^2 = \frac{e_0^2}{\epsilon\epsilon_0 k_B T} \sum_i n_i z_i^2 \tag{19}$$

Here e_0 is the elementary charge, ϵ the dielectric constant of water, k_B the Boltzmann constant, and T the temperature. The different number concentrations of the small ions are denoted by n_i and their charge by z_i = ± 1 for the case of monovalent ions. The ionic strength of the solution is defined as

$$I = \frac{1}{2} \sum_i n_i z_i^2 \tag{20}$$

The MC simulations are restricted in this study to the concentration regime $c \leq 4c^*$. A more detailed description of the underlying model is given in a previous paper.[25]

To fit the experimental data by the MC results, the added salt concentration n_{salt} has to be inserted. The actual concentration n_{salt} is estimated from electric conductivity measurements. Assuming all ions to move independently at low ionic strength ($\approx 10^{-5}$ M) the conductivity σ_{total} is given by

$$\sigma_{total} = n_{salt} e_0 (\mu_{Na} + \mu_{Cl}) + \sigma_{particle} \tag{21}$$

The mobilities μ_{Na} and μ_{Cl} are taken from literature. The last term $\sigma_{particle}$ of eq 21, representing the macroion and their counterion contribution to the conductivity, may be approximated as the measured conductivity of the correspondent zero salt solution; n_{salt} is then deduced from

$$n_{salt} = \frac{\sigma_{total} - \sigma_{particle}}{e_0(\mu_{Na} + \mu_{Cl})} \tag{22}$$

The conductivity due to the concentration of OH⁻ ions can be calculated from the dissociation product of water and is found to be negligible.

3. Experimental Section

3.1. Sample Preparation. All the samples in this study were kindly supplied by Prof. C. Wetter (Universität Saarbrücken, FRG). The various concentrations used for SLS were obtained by diluting the stock solution of TMV particles (c = 53 mg/mL; length, L = 300 nm; diameter, d = 18 nm; MW = 4.0×10^7) with highly deionized water (18 MΩ·cm). These samples were filtered several times through a 0.45-μm Millipore filter and stored over mixed-bed ion-exchange resin MB3 (Serva, FRG). To eliminate dust and other large particles, the samples were centrifuged at 1000 rpm between 20 and 120 min before further use. The actual concentrations of the samples were determined by their UV absorption at λ = 260 nm with an absorption coefficient of 3.06 (1 mg/(mL·cm)), using a Beckmann spectrometer (DU-64, FRG).

Table I
Overview of Samples Used in the Neutron Scattering Investigations

sample TMV/H_2O	added salt concn	concn (mg/mL)	particle concn, ($\times 10^{14}$/mL)	c/c^* (c^* = 2.45 mg/mL)
		Series 1		
1		26.7	4.00	10.89
2		21.8	3.29	8.9
3		14.3	2.16	5.84
4		13.1	1.97	5.34
		Series 2		
5	2 mM Tris-HCl	31.0	4.50	12.15
6	"	28.6	4.32	11.67
7	"	22.9	3.45	9.34
8	"	12.1	1.83	4.94
		Series 3		
9	8 mM Tris-HCl	65.0	9.81	26.53
10	"	57.5	4.32	11.67
11	"	44.6	6.92	18.70
12	"	28.7	4.33	11.71
13	6 mM Tris-HCl	11.2	1.69	4.57

For the SANS experiments three series of TMV concentrations at different ionic strengths given in Table I were prepared. Sample no. 13 of c = 11.2 mg/mL and an ionic strength of 6 mM Tris-HCl was used for the form-factor measurement. To keep the particle charge at its maximum value, two samples were prepared at pH = 8 by a dialyzing procedure using a Tris-HCl buffer solution of 2 and 8 mM. Both samples separate into an isotropic and a nematic liquid-crystalline phase. The concentrations were measured as $c_{isotropic}$ = 35.2 mg/mL and $c_{nematic}$ = 46.5 mg/mL for the 2 mM solution and $c_{isotropic}$ = 65 mg/mL and $c_{nematic}$ = 82.8 mg/mL for the 8 mM solution. The coexistence concentrations are close to the previously determined values for well-characterized monodisperse samples.[12] From the isotropic part of each sample a stock solution is extracted to obtain the four diluted concentrations of series 2 and 3, respectively. In this way any long-range orientational correlation of the investigated samples can be excluded. The samples of series 1 were obtained in an analogous way but without dialyzing and using highly deionized water instead of buffer solution. The monodispersity of all samples was checked by an analytical centrifuge and magnetic field induced birefringence measurements at the Max-Planck-Institut für Festkörperphysik, Hochfeld-Magnetlabor, Grenoble, France. The results are in good agreement with the data recently published by Fraden et al.[12]

3.2. Light Scattering. For the measurements a light scattering apparatus (ALV, FRG) was used consisting of a computer-controlled goniometer table with focusing and detector optics and a power-stabilized 3-W argon ion laser (Spectra Physics), a digital ratemeter, and a temperature control which stabilized the temperature of the sample cell at T = 21 ± 1 °C. Measurements and data acquisition were controlled by a personal computer. Intensity data were corrected by the dark rate of the photomultiplier and by the angle dependence of the scattering volume. The magnitude of the scattering vector

$$q = \frac{4\pi n_s}{\lambda} \sin\frac{\theta}{2}$$

ranges from 0.3×10^{-2} to 3.3×10^{-2} nm^{-1}, at the laser wavelength λ = 488 nm in aqueous solutions with a refractive index n_s = 1.33. The beam first passed an index match fluid (silicon oil) and then entered the scattering cell, where it is focused into the scattering volume. For the scattering cells, we used quartz tubes of 10-mm outer diameter.

To control the ionic strength of the sample, the scattering cell was installed in a closed-tube circuit (Figure 2) using a modified technique of Palberg and Härtl.[26] The centrifuged samples were transferred into the sample reservoir. Further elements of the circuit are a conductivity cell, a pH electrode placed in the sample reservoir, a tube pump, and a column of ion-exchange resin. To
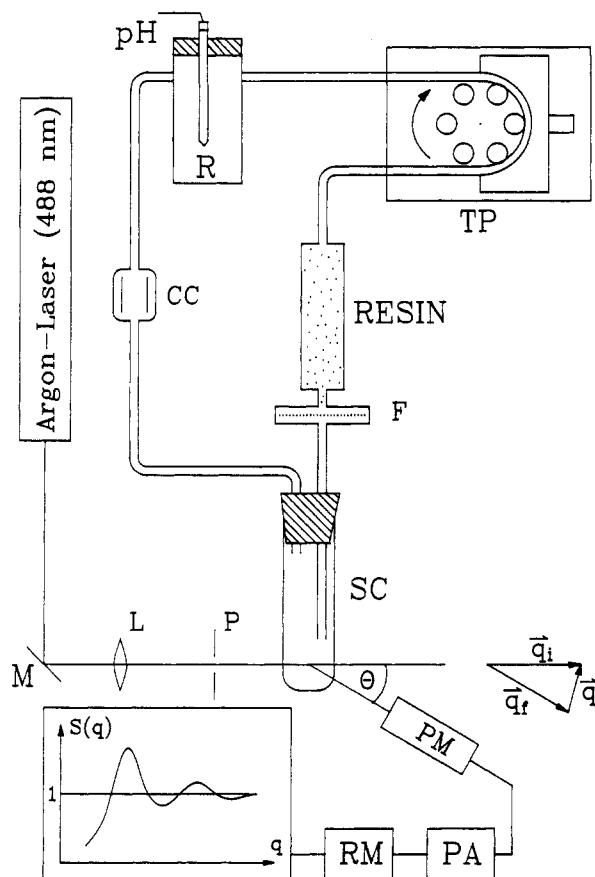

Figure 2. Closed-tube circuit is installed into the SLS apparatus: TP = tube pump, RESIN = ion-exchange resin, F = filter (5 μm), SC = scattering cell, CC = conductivity cell, pH = pH meter, R = sample reservoir. The SLS apparatus consists of the following: Argon-Laser, M = mirror, L = lens (f = 60 mm), P = pinhole, PM = photomultiplier, PA = preamplifier, RM = ratemeter.

keep the scattering cell clean of resin particles, a 5-μm filter is fixed at the end of the column. The ionic strength is increased by adding salt and decreased by pumping the solution through the column.

All measurements were normalized to a reference sample (toluene) in the total q region to correct laser power fluctuations and to get a standard of the incident light intensity.

3.3. Small-Angle Neutron Scattering. Experiments were carried out on the neutron small-angle diffraction instrument D11 at the Institut Laue-Langevin in Grenoble with neutrons of wavelength λ = 7 Å. The scattered intensity was recorded with a two-dimensional multidetector of 64 × 64 cells of 1-cm^2 area. Five sample-detector distances were used: 2.5, 5, 10, 20, and 35.3 m, all with a constant collimation distance of 10 m. The samples were thermostated at a temperature of 21 °C.

Following the documented normalization procedure of Ghosh,[27] each data set consisting of the $I(q)$ files at the five detector distances is then reduced to obtain the coherent intensity scattered by the TMV particles (eq 10). After treating the set of five files in this manner they were fitted together to correct for any differences in intensities due to the different sample to detector distances.

4. Results and Discussion

4.1. SANS. All samples investigated by SANS are given in Table I. Typical scattered intensity curves as a function of the concentration are shown in Figure 3 as a function of q in the case of series 1, the lowest ionic strength examined. The pronounced maxima of the scattered intensities give evidence for strong interparticle correlations. The positions of the maxima are shifted with increasing particle concentration to larger q values. In
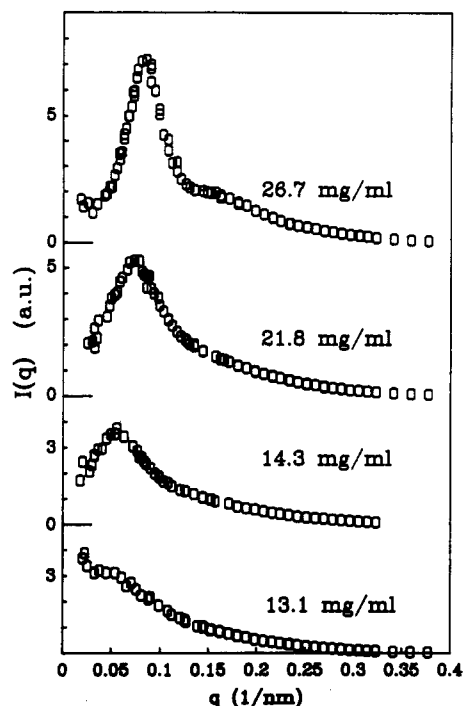
Figure 3. Scattered intensities by SANS of the TMV samples of series 1 as given in Table I. With increasing concentration a pronounced intensity maximum is found.
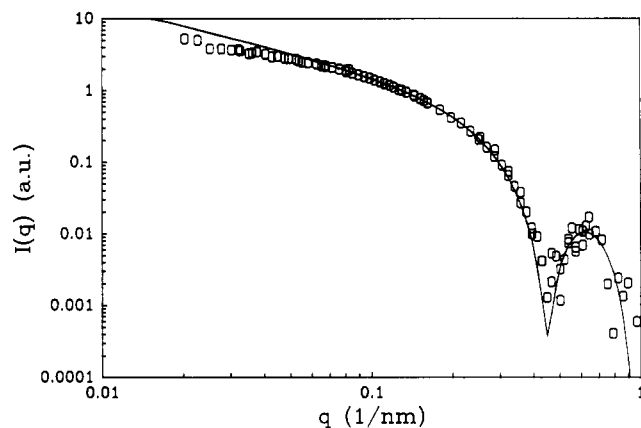

Figure 4. Calculated TMV form factor (—) of an isotropic solution given by eq 16 compared to the experimental form factor of sample 13 as measured by SANS.

the following sections the static structure factors are derived from the scattered intensities of all samples.

Absence of birefringence assures that the solutions form an isotropic phase, and therefore the orientation distribution of the rods is isotropic on a macroscopic scale. Measurements of the magnetic field induced birefringence at the Hochfeld-Magnetlabor, MPI für Festkörperforschung, Grenoble, indicate local angular correlations between the TMV rods in agreement with the results recently published by Fraden et al.[12] As the scattering experiments measure an isotropic average of the angular correlations, the theoretical form factor of eq 16 may be used to fit the experimental data in the high q region where the static structure factor equals 1. Figure 4 shows the form-factor measurement given by the scattered intensity of sample 13 which is prepared with low particle concentration and high ionic strength to exclude particle interactions due to Coulombic repulsion. The experimental result is in good agreement with the theoretical form factor of isotropically oriented hollow rods calculated with the rod parameters $L = 300$ nm, $R_i = 2$ nm, and $R_a = 8$ nm.
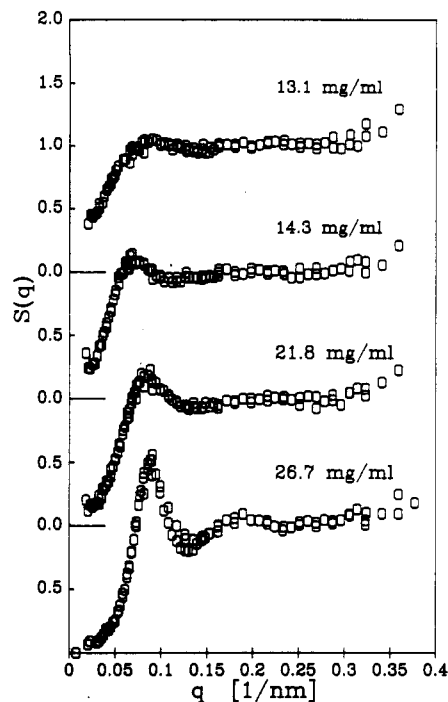

Figure 5. Static structure factor of the TMV samples of series 1 obtained by SANS.

The deviation in the low q region is assumed to be caused by steric interaction of the particles.

All scattering intensities are normalized by concentration and by the scattering amplitude $d\sigma_0/d\Omega$. To derive the static structure factors, a decoupling between angular and spatial correlations is assumed. $S(q)$ is then given by eq 11 inserting the experimental form factor. Three series of different ionic strengths as defined in Table I were chosen to measure the $S(q)$ over the adequate concentration regime of the isotropic phase.

The ionic strength of series 1 is given by the H_3O^+ concentration which is not exactly known. As the degree of dissociation of the particles' acid surface groups depends on the pH value of the solution, an increase of the particle concentration leads to a decrease of the particle charge number. Only if the pH value is buffered in the range of pH 7–8 will the charge number take its maximum value of 1–2 elementary charges per protein subunit.[24,28] Therefore, in any case, the small ion concentration of each sample of series 1 is smaller than 1 mM. As a function of the particle concentration, Figure 5 shows the static structure factors. With increasing particle concentration the interaction becomes stronger and a characteristic liquidlike structure is formed. Particularly pronounced at $c = 26.7$ mg/mL, a first maximum with a peak height of about 1.56 is followed by a second maximum. In the low q region the scattered intensity strongly decreases due to the decrease of the osmotic compressibility, whereas at large q values $S(q)$ equals 1.

Series 2 and 3 were prepared with added salt concentrations of 2 and 8 mM Tris-HCl buffer at pH = 8.0. The actual small ion concentration screening the macroion charge is given by the added salt and the H_3O^+ counterion concentration. Figure 6 illustrates the corresponding static structure factors of series 3. The samples of series 2 (see Table II) give similiar results. Due to the larger screening the peak heights take only values of about 1.15, i.e., the liquidlike structure is much less pronounced compared to series 1. In Tables II and III discussed below, we compare the Debye screening length κ^{-1} of the different samples with the experimental "probe distance" $d_{probe} = 2\pi/q_{max}$.
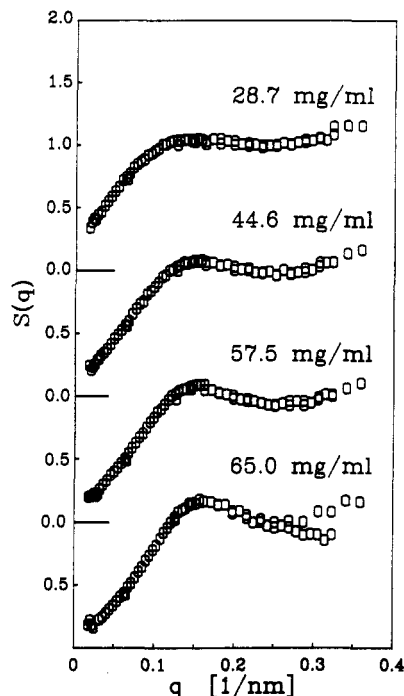
Figure 6. Static structure factor of the TMV samples of series 3 obtained by SANS. Even at the concentration of 65 mg/mL = 26.5c/c^* a liquidlike structure is found.

Table II
Properties of Samples Used in the Neutron Scattering Investigations

sample TMV/H$_2$O (mg/mL)	concn of small ions (mM)	q_{max} (1/100 nm)	$S(q_{max})$	$r_{max} = 2\pi/q_{max}$ (nm)	κ^{-1} (nm)	r_{max}/κ^{-1}
Series 1						
1 (26.7)	≤1	8.79	1.56	71.5	≥13.84	≤5.17
2 (21.8)	≤1	8.30	1.16	75.7	≥13.84	≤5.17
3 (14.3)	≤1	6.80	1.10	92.4	≥13.84	≤5.17
4 (13.1)	≤1				≥13.84	
Series 2						
5 (31.0)	4.75	11.7	1.15	53.7	6.34	8.47
6 (28.6)	4.72	11.4	1.12	55.1	6.36	8.66
7 (22.9)	4.57	10.3	1.07	61.0	6.46	9.40
8 (12.1)	4.30				6.66	
Series 3						
9 (65.0)	17.63	15.9	1.18	39.8	3.29	12.09
10 (57.5)	17.44	15.3	1.09	41.0	3.31	12.38
11 (44.6)	17.15	14.8	1.08	42.4	3.33	12.73
12 (28.7)	16.72				3.38	
13 (11.2)	12.28				3.94	

Table III
Properties of the Sample Used in the Light Scattering Investigations for the Determination of the Ionic Strength Dependence of the Static Structure Factor

σ_{total} (μS)	n_{salt} (M)	$S(q_{max})$	q_{max} (1/nm)	$r_{max} = 2\pi/q_{max}$ (nm)	κ^{-1} (nm)	r_{max}/κ^{-1}
1.62	0.0	2.16	0.0189	332.4	127.6	2.61
2.51	6.48 × 10⁻⁶	1.87	0.0194	323.8	86.7	3.73
3.3	1.27 × 10⁻⁶	1.60	0.0197	318.9	70.8	4.50
4.4	2.14 × 10⁻⁵	1.35	0.0205	306.5	58.2	5.26
5.5	3.01 × 10⁻⁵	1.26	0.0209	300.6	50.7	5.93
6.9	4.11 × 10⁻⁵	1.14	0.0220	285.6	44.3	6.44
9.95	6.53 × 10⁻⁵	1.06	0.0246	255	36	7.09
13.7	1.00 × 10⁻⁵				27.1	

For the buffered samples κ^{-1} is calculated assuming the particle charge to be fixed at 1000e. It is well below the maximum value from literature of 1–2e per protein subunit, taking into account the effect of counterion condensation.[29] For the unbuffered samples this estimation may be
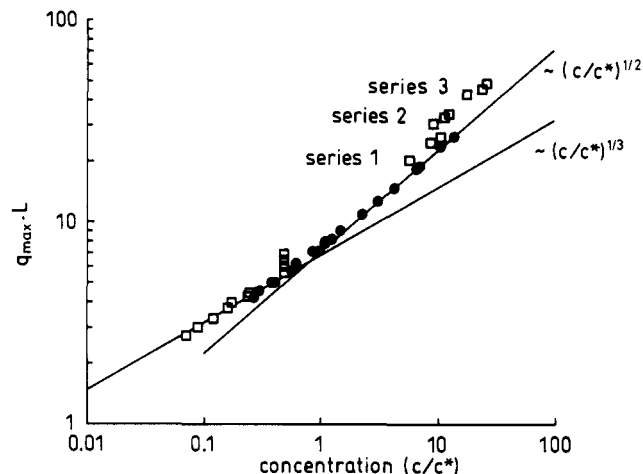

Figure 7. Position q_{max} of the maximum of $S(q)$ as a function of the particle concentration for TMV (□) and fd solutions (●). The TMV results are obtained by SLS for $c < c^*$ and by SANS (see Table I) for $c > c^*$. All fd results are obtained by SLS.[18] Below $c = c^*$ the data are fitted by $q_{max} \sim (c/c^*)^{1/3}$ (see eq 23) and above $c = c^*$ by $q_{max} \sim (c/c^*)^{1/2}$ (see eq 24).

considered as the upper possible value. At small macroparticle concentrations the ratio d_{probe}/κ^{-1} may serve as a measure of spatial particle–particle correlations, provided the particle charge is constant. The calculated values show that even at $c \gg c^*$ the ratio d_{probe}/κ^{-1} is found to be minimal in the case of strongest liquidlike order.

The SANS investigations extend the concentration range limited so far by SLS[16] to $c < c^*$ into the semidilute regime $c > c^*$ and concentrated regime $c \gg c^*$. In Figure 7 all available data with regard to the position of the maximum of $S(q)$ are plotted versus relative concentration c/c^* for $0.04 < c/c^* < 26.5$. Additionally, the fd results are included. The experimental data are fitted by

$$q_{max}L = 2\pi 1.09(c/c^*)^{1/3} \qquad (23)$$

for $c < c^*$ and

$$q_{max}L = 2\pi 1.13(c/c^*)^{1/2} \qquad (24)$$

for $c > c^*$. The q_{max} values of the TMV solutions are close to the straight line of Figure 7, which according to eq 24 is appropriate to fit the fd data. The deviations from $q_{max} \sim c^{1/2}$ of eq 24 toward higher q_{max} values are associated with the fact that at fixed macroion concentration the position of the static structure factor maximum depends on the screening ion concentration. This behavior is theoretically and experimentally known for interacting spherical particles[4,6,19] and is discussed in detail in section 4.2. Equation 23 is known from solutions of spherical particles. It can also be applied to rodlike macroparticles well below c^*, where the latter approximately can be regarded as pointlike polyions.[18,25] The fit parameter 1.09 is directly related to the number of nearest neighbors. Around and above c^* the interaction between the macroparticles is affected by the anisotropic particle geometry. This is clearly shown by MC simulations.[18,25] In this context the static structure factor is written as

$$S(q) = 1 + \sum_{l_1 l_2 l} S(l_1 l_2 l; q) \qquad (25)$$

See eq 17 of ref 25. The first term, $S(000,q)$ arising from the center-to-center correlations, describes the measured static structure factor correctly at concentrations $c \ll c^*$. Its maximum decreases strongly above $c > 2c^*$. The corresponding wavevector shifts below the overlap concentration exactly as $q_{max} \sim c^{1/3}$. In contrast, the contribu-

tions to $S(q)$ from the terms $S(l_1l_2l,q)$ with $l_1l_2l > 0$, negligible at $c \ll c^*$, become more and more important with increasing concentration and are responsible for the turnover to the $c^{1/2}$ scaling of q_{max}. Thus, $2\pi/q_{max}$ does not describe any longer a preferred distance between centers of gravity above c^* but a somewhat larger value. The system of charged rods remains globally isotropic as required by the absence of birefringence. Regarding correlations of the nearest-neighbor rods, a tendency to parallel alignment is observed with a local ordering parameter $S = 0.075$ at $c = 2.29c^*$.[18] The MC results have been compared to light scattering results from fd particles.[17] Good agreement has been achieved up to $c = 2.29c^*$.

Summarizing, this means that there is no local ordering of rods up to this relative concentration, but the q_{max} value of the static structure factor already obeys the $c^{1/2}$ dependence (Figure 5 of ref 18). Unfortunately, the SANS results refer to $c \geq 5c^*$ where MC simulations could not be performed yet. However, the available results seem to indicate that the rods do not necessarily have to be parallel to each other, not even in small correlation volumes, to describe the $c^{1/2}$ law of q_{max} above c^* and below the transition to the nematic phase, although we cannot exclude this possibility completely. Two idealized models predicting the scaling of q_{max} as $c^{1/2}$ have been discussed in the literature.[30,31] The first is a cubic array of mutual perpendicular rods of great length to diameter ratio and the second the packing of long parallel rods on a hexagonal lattice. At low concentrations of $c \approx c^*$, where both the orientational entropy and electrostatic repulsion terms in the free energy expressions of a suspension of charged rods favor antiparallel alignment of rods, we expect the cubic array is the appropriate simple model of interparticle structure. While at higher concentrations, closer to the isotropic to nematic phase transition where the packing entropy term dominates interparticle correlations, we expect the hexagonal packing of parallel rods to be the appropriate model.[32] The models satisfy two conditions which we conjecture to be fulfilled at $c \gg c^*$. First, the separation between particles has to be much less than their length, so that the rods can be considered as infinitely long. Second, because the rods are charged they want to have surfaces which are separated as far apart as possible. Both models predict that q_{max} scales as $c^{1/2}$ with

$$q_{max}L = 2\pi\beta(c/c^*)^{1/2} \qquad (26)$$

with $\beta = 0.58$ for the cubic structure and $\beta = 0.93$ for the hexagonal case. Considering the gross oversimplifications of these models, the prefactors are close to the experimental value.

4.2. Static Light Scattering. In order to explain the shift of the q_{max} data from the straight line in Figure 7, it would be necessary to have a quantitative relation between q_{max} and the salt concentration n_{salt}. As stated before such a theory is not available yet and also MC simulations cannot be used at these high macroion concentrations. Therefore we shall confine ourselves here to the SLS concentration regime and then compare our results to the SANS regime.

Previous investigations of the liquidlike phase of spherical or rodlike particles gave no quantitative correlation between the formation of the static structure factor and the ionic strength of the system. Using a new closed-tube circuit technique described in section 3.2, we present SLS measurements at a fixed macroion concentration as a function of the ionic strength. This method allows the salt concentration to be reproducably varied at small steps even at ionic strengths well below $I = 10^{-3}$ M which cannot
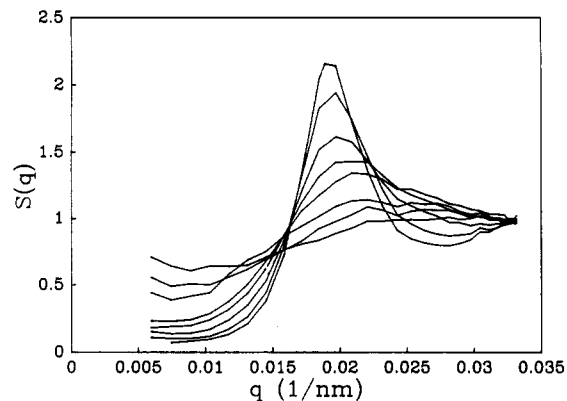

Figure 8. Static structure factor obtained by SLS of a TMV sample of $c = 0.53 c^*$ as a function of the measured conductivity σ_{total} of the solution. σ_{total}, which is controlled by the closed-tube circuit, is proportional to the salt concentration. The maximum of the $S(q)$ increases with decreasing conductivity. The corresponding values of σ_{total} and $S(q_{max})$ are given in Table III.

be achieved by the dializing procedure or by adding small amounts of salt.

We choose a TMV sample of 1.29 mg/mL ($0.53c^*$) to determine the static structure factor as a function of the electric conductivity of the solution. Again no optical birefringence is found, and $S(q)$ is calculated by eq 1 (see Figure 8). At the minimal conductivity, reached at $\sigma_{total} = 1.62$ μS/cm, all NaCl ions are removed by the ion-exchange procedure. A liquidlike order is formed, and the peak height of $S(q)$ takes a maximum value of about 2.1. By adding salt the influence of the screening ions leads to a decrease of the peak height and to a shift of the first-maximum position q_{max} to larger q values. Finally, at a measured conductivity of $\sigma_{total} = 13.7$ μS/cm the first maximum vanishes.

In colloidal suspensions this shift of q_{max} due to the increasing ionic strength is a characteristic feature and is also found in spherical particle systems. In this case it is possible to give an interpretation in terms of the radial pair distribution function $g(r)$. In a solution of interacting latex spheres of radius $a = 50 \pm 1$ nm and a concentration $c = 0.1$ vol % the static structure factor is measured as a function of the salt concentration and is compared to calculations by the hypernetted chain approximation (HNC) which yields $S(q)$ and $g(r)$ as well. Qualitively as shown in Figure 9 the effect on $S(q)$ is the same as that observed in the system of interacting rodlike TMV particles. The radial pair distribution function $g(r)$ in Figure 10 calculated for each salt concentration shows that the distance of neighboring particles given by

$$r_{max} = n_{neighbor}c^{-1/3} \qquad (27)$$

at low ionic strength is affected in the following way. As the weakening of the Coulombic repulsion allows the particles to penetrate into previously excluded interparticle space, the distance r_{max} decreases. In the first shell of neighboring particles a rearrangement takes place. For the zero salt solution the first-maximum position of $g(r)$ takes a value of $r_{max} = 846$ nm whereas at a salt concentration of $n_{salt} = 1.1 \times 10^{-5}$ M a value of $r_{max} = 645$ nm is found. In eq 27 this can be expressed by a salt-dependent coefficient $n_{neighbor}$ which is related to the number of nearest neighbors.[6] Consequently the pair distribution function is changing toward a simple step function as is found in the case of pure hard-core interaction. This can be shown theoretically in the limit of $n_{salt} \rightarrow \infty$.[33]
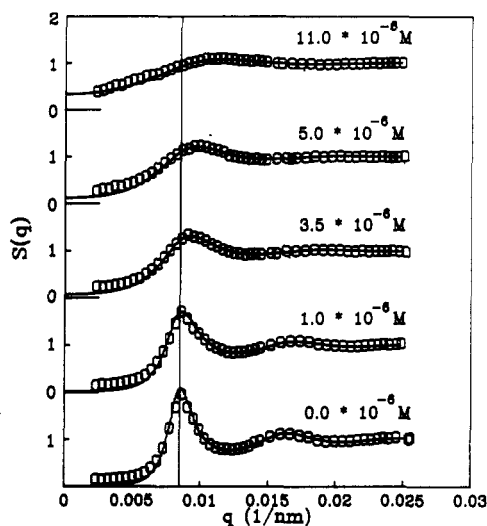
Figure 9. Static structure factor obtained by SLS of a solution of monodisperse 50-nm latex spheres as a function of the salt concentration (NaCl). (—) Calculated $S(q)$ by HNC approximation.
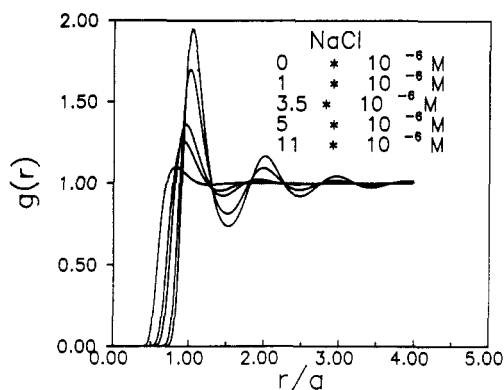

Figure 10. Radial pair distribution function $g(r)$ calculated by the HNC approximation for the solution of latex spheres shown in Figure 9. With increasing ionic strength ($0.0-11 \times 10^{-6}$ M) the first maximum of $g(r)$ decreases and is shifted to lower values of r/a.

For the MC simulations of the TMV samples the only fit parameter inserted is the particle charge of $Q = 360e$ whereas the TMV concentration and the salt ion concentration n_{salt} are taken from the experiments. Assuming all ions to move independently, the actual value of n_{salt} can be calculated from the measured conductivities σ_{total} and $\sigma_{particle}$ according to eq 22. MC results and experiments as shown in Figure 11 are in good agreement, confirming the modeled interaction potential and the salt concentration n_{salt} derived in this way. No indication of local and global ordering of the rod axes is found, and the position q_{max} of the first maximum in $S(q)$ is in agreement with the $c^{1/3}$ law of eq 23.[16,18] The deviations of q_{max} with increasing n_{salt} have to be compared to the q_{max} positions in the SANS regime. Although we are at present not able to extend the Monte Carlo simulations to these high concentrations, it seems obvious that those measurements have to be interpreted in the same way. The too high values compared with the straight line in Figure 7 will very likely be reduced to the latter.

The Monte Carlo results yield a quantitative correlation (Table III) between the strength of liquidlike order as defined above and the ionic strength of the solution. The formation of the static structure factor is controlled only by the Debye screening length. As soon as κ^{-1} exceeds the value of 36 nm for the given concentration of $c = 0.53c^*$
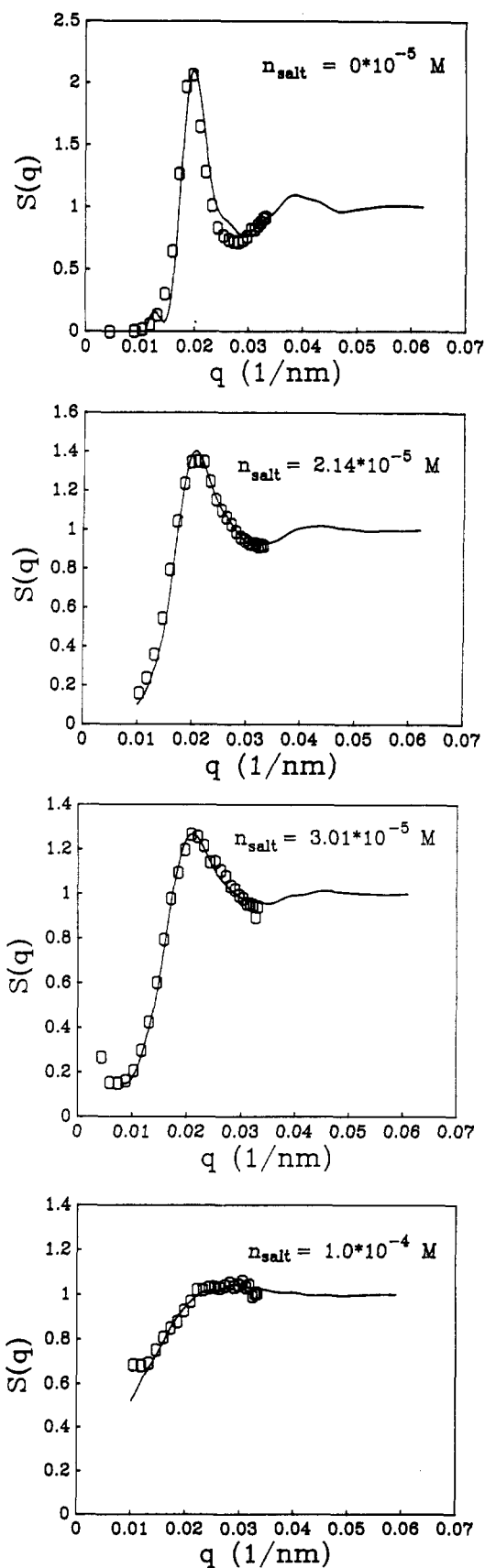

Figure 11. Static structure factor obtained by SLS of the TMV sample shown in Figure 8 compared to the MC results (—). With increasing salt concentration $S(q_{max})$ decreases as given in Table III.

the onset of the interparticle correlations is observed. The peak height is growing up to its maximum value of about 2.1 as κ^{-1} is increased to 127 nm. This is the case of strongest overlap of the particles repulsive Coulombic potential. No

further increase of interparticle interaction is possible because all other ions but H_3O^+ have been exchanged. Therefore no phase transition to a nematic or liquid-crystalline phase is possible.

5. Conclusions

In this work we have investigated the formation of interparticle correlations in a rodlike particle system as a function of the macroparticle concentration and the ionic strength of the solution. The static structure factor of TMV solutions in the isotropic phase is determined by SLS and SANS well below and above the overlap concentration c^*. The SANS results show that the liquidlike phase exists even at concentrations of about $25c^*$.

Previous results from SLS experiments and MC simulations indicate a crossover in the scaling behavior of the first-maximum position with concentration due to the influence of the particle's anisotropy. This crossover has been shown to occur indeed for a single system, thus confirming the indicated behavior of the fd data. We conclude that this is characteristic for any system of charged rodlike particles. On the basis of the results from SLS measurements below c^*, we associate the deviations of the SANS data for $c \gg c^*$ from eq 26 to a change in potential due to the screening of small ions. By SLS and HNC investigations of the spherical particle system we show that this shift in q_{max} corresponds unequivocally to a shift in r_{max} of $g(r)$. Transferred to the rodlike particle system this means that the TMV particles can now interpenetrate into previously excluded volume and a rearrangement of the first shell of nearest neighbors takes place.

References and Notes

(1) Brown, J. C.; Pusey, P. N.; Goodwin, J. W.; Ottewill, R. H. *J. Phys. A* **1975**, *8*, 664.
(2) Grüner, F.; Lehmann, W. *J. Phys. A* **1979**, *12*, L303.
(3) Grüner, F.; Lehmann, W. *J. Phys. A* **1982**, *15*, 2847.
(4) Härtl, W.; Versmold, H.; Wittig, U.; Marche, V. *Mol. Phys.* **1983**, *50*, 815.
(5) Okubo, T. *J. Chem. Phys.* **1989**, *90*, 2408.
(6) Tata, B. V. R.; Kesavamoorthy, R.; Arora, K. A. *Mol. Phys.* **1986**, *57*, 363.
(7) Carlson, R. J.; Asher, S. A. *Appl. Spectrosc.* **1984**, *38*, 297.
(8) Onsager, L. *Ann. N.Y. Acad. Sci.* **1949**, *51*, 627.
(9) Stroobants, A.; Lekkerkerker, H. N. W.; Odijk, T. *Macromolecules* **1986**, *19*, 2232.
(10) Lee, S.; Meyer, R. B. *J. Chem. Phys.* **1986**, *84*, 3443.
(11) Frenkel, D. *J. Chem. Phys.* **1988**, *92*, 3280.
(12) Fraden, S.; Maret, G.; Caspar, D. C. D.; Meyer, R. B. *Phys. Rev. Lett.* **1989**, *63*, 2068.
(13) Kaji, K.; Urakawa, H.; Kanaya, T.; Kitamaru, R. *J. Phys. Fr.* **1988**, *49*, 993.
(14) Drifford, M.; Dalbiez, J. P. *J. Phys. Chem.* **1984**, *88*, 5368.
(15) Krause, R.; Maier, E. E.; Deggelmann, M.; Hagenbüchle, M.; Schulz, S. F.; Weber, R. *Phys. A* **1989**, *160*, 135.
(16) Maier, E. E.; Schulz, S. F.; Weber, R. *Macromolecules* **1988**, *21*, 1544.
(17) Schulz, S. F.; Maier, E. E.; Weber, R. *J. Chem. Phys.* **1989**, *90* (1), 7.
(18) Hagenbüchle, M.; Weyerich, B.; Deggelmann, M.; Graf, C.; Krause, R.; Maier, E. E.; Schulz, S. F.; Klein, R.; Weber, R. *Phys. A* **1990**, *169*, 532.
(19) Nägele, G.; Klein, R.; Medina-Noyola, N. *J. Chem. Phys.* **1985**, *83*, 2560.
(20) Berne, J. B.; Pecora, R. *Dynamic Light Scattering*; John Wiley and Sons, Inc.: New York, 1976.
(21) Schneider, J.; Karrer, D.; Dhont, J. K. G.; Klein, R. *J. Chem. Phys.* **1987**, *87*, 3008.
(22) Schneider, J.; Hess, W.; Klein, R. *J. Phys. A: Math. Gen.* **1985**, *18*, 1221.
(23) Caspar, D. L. D. *Adv. Protein Chem.* **1963**, *18*, 37.
(24) Franklin, R. E.; Caspar, D. L. D. *Nature* **1956**, *177*, 928.
(25) Weyerich, B.; D'Aguanno, B.; Canessa, E.; Klein, R. *Faraday Discuss. Chem. Soc.* **1990**, *90*, 245.
(26) Deggelmann, M.; Palberg, T.; Hagenbüchle, M.; Maier, E. E.; Krause, R.; Graf, C.; Weber, R. *J. Colloid Interface Sci.* **1991**, *143*, 318.
(27) Ghosh, R. E. *A Computing Guide of Small Angle Scattering Experiments*; Institute Laue-Langevin: Grenoble, France, 1989.
(28) Fankuchen, I.; Bernal, J. B. *J. Gen. Physiol.* **1941**, *25*, 111.
(29) Manning, G. S. *Q. Rev. Biophys.* **1978**, *11*, 179.
(30) de Gennes, P.-G.; Pincus, P.; Velasco, R. M. *J. Phys. (Paris)* **1976**, *37*, 1461.
(31) Isenberg, G.; Schmidt, C. F.; Baermann, M.; Sackmann, E. *Macromolecules* **1989**, *22*, 3638.
(32) Odijk, T. *Macromolecules* **1986**, *19*, 2313.
(33) Nägele, G. *Zur Statik und Dynamik von binären Mischungen geladener Brownscher Teilchen.* Ph.D. Thesis, Universität Konstanz, 1987.